



HAL
open science

Manipulation planning with contacts for an extensible elastic rod by sampling on the submanifold of static equilibrium configurations

Olivier Roussel, Andy Borum, Michel Taïx, Timothy Bretl

► **To cite this version:**

Olivier Roussel, Andy Borum, Michel Taïx, Timothy Bretl. Manipulation planning with contacts for an extensible elastic rod by sampling on the submanifold of static equilibrium configurations. IEEE International Conference on Robotics and Automation (ICRA 2015), May 2015, Seattle, United States. hal-01096543v2

HAL Id: hal-01096543

<https://hal.science/hal-01096543v2>

Submitted on 10 Mar 2015

HAL is a multi-disciplinary open access archive for the deposit and dissemination of scientific research documents, whether they are published or not. The documents may come from teaching and research institutions in France or abroad, or from public or private research centers.

L'archive ouverte pluridisciplinaire **HAL**, est destinée au dépôt et à la diffusion de documents scientifiques de niveau recherche, publiés ou non, émanant des établissements d'enseignement et de recherche français ou étrangers, des laboratoires publics ou privés.

Manipulation planning with contacts for an extensible elastic rod by sampling on the submanifold of static equilibrium configurations

Olivier Roussel¹, Andy Borum², Michel Taïx¹ and Timothy Bretl²

Abstract—We consider the manipulation planning problem of an extensible elastic rod in collision-free or contact space. We assume the rod can be handled by grippers either at both or at only one of its extremities and during the manipulation, the grasped end may change. We show that the use of both quasi-static and dynamic models can be coupled efficiently with sampling-based methods. By sampling directly on the submanifold of static equilibrium and contact-free configurations, we can take advantage of the dynamic model to improve the exploration in the state space. We show the necessity of considering contacts for this type of problems with several simulation experiments on various scenarios.

I. INTRODUCTION

Motion planning plays an essential role in assembling and disassembling industrial cases. Approaches have been proposed to the extension of this problem to robots manipulating movable rigid objects [15]. Moreover, in the automotive or aeronautical industry, manipulating deformable parts is necessary. In this context, most of these consist in circular Deformable Linear Objects (DLOs) (cable, hose, pipe,...) and are usually referred as rods in the mechanical literature. In the classical motion planning problem formulation, the objective is to compute a path in the collision-free space, without contacts, but in realistic conditions for this context the contact is actually a necessary condition.

In this paper, we consider the manipulation planning problem of a rod in free or contact space (as in Figure 1). We assume the rod is handled by a gripper at one of its extremities and the grasped end may change during the manipulating phase. As rod can be geometrically interpreted as an infinite-dimensional continuous curve, planning in the discretization of this curve may lead to high finite-dimensional configuration spaces. Furthermore, identifying the manifold of feasible configurations, i.e. which satisfy mechanical constraints, on this configuration space is a challenging task. This is even more difficult if also considering both dynamics of the rod and contacts.

Some work has been done using the reasonable assumption of considering only the collision free space of quasi-static configurations. These approaches are based on the numerical minimization of the total elastic energy for given gripper placements [9], [11], [18].

An approach to the manipulation planning considering dynamics of the rod and contacts is to plan in the finite space

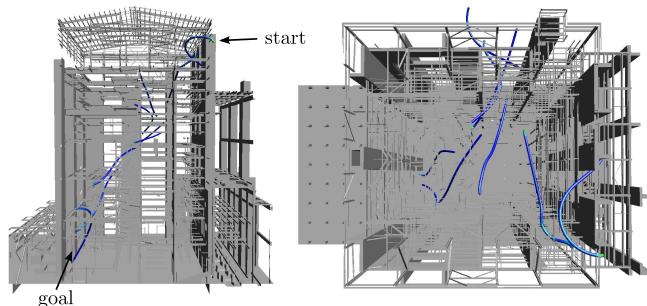


Fig. 1. Solution path for an elastic rod to the "powerplant" scenario. Both sides (left) and top (right) views have been clipped for clarity.

of controls for a given number of grippers. In this case, the state transition function is assumed to be known and can be delegated, for example, to a simulator. For a physically realistic rod model, these might use complex finite elements methods resulting in computationally expensive local planning schemes. For instance, the motion planning problem for deformable objects has been addressed in [12] which coupled a deformable dynamics model with a kinodynamic motion planning algorithm. However, the use of fully deformable environments prevents the robot to be stuck in local minima and bypasses the local control problem.

In [14], the manipulation planning problem of a DLO is addressed from a topological perspective by focusing on knot tying application with the help of many grippers.

More generally, the motion planning problem for deformable objects has already been investigated, especially in the case of simplified visually realistic deformation models. For example, [3] extended the Probabilistic Roadmap Methods (PRMs) [2] for deformable objects by reducing the deformation space to a one dimensional one. [6] used the Constraint Based Motion Planning framework to simulate a deformable robot along a guide path computed for a point-like robot. This work has then been extended to the specific class of DLOs in [7].

Recent results based on the local solution of a geometric optimal control problem enabled to define this configuration space [5], where it is shown this space defines a finite dimensional manifold that can be parameterized by a single chart. In previous work [13], we presented a motion planning algorithm for a quasi-static inextensible elastic rod in complex environments and we showed that quasi-static solution paths in the collision-free space can be computed efficiently by assuming the rod as handled by both extremities. However, slight changes in grippers wrenches involve a change

¹CNRS, LAAS, Univ. de Toulouse, UPS, 7 avenue du Colonel Roche, F-31400 Toulouse, France, roussel@laas.fr, taix@laas.fr

²Department of Aerospace Engineering, University of Illinois at Urbana-Champaign, Urbana, IL 61801, USA, borum2@illinois.edu, tbretl@illinois.edu

of the whole rod shape which causes greater probability of collision. Consequently, in constrained environments, the roadmap suffers from a slow growth of rate.

On the other hand, the physical engine eXtended Dynamic Engine (XDE) offers a realistic multi-body dynamics simulation with contact for deformable bodies. Thus, XDE can compute dynamic motions but at the cost of a high computational time, conflicting with random motion planning needs. However, it seems interesting to allow sliding along the contact space to improve significantly the exploration.

In this context, we can define a manipulation planning approach based on sampling-based methods. By sampling on the submanifold of quasi-static contact-free configurations, it is then possible to use dynamic simulation to extend the exploration of the state space. Using a parameterization to sample directly on the submanifold, we can limit the number of calls to the simulator to extension steps and to take advantage of provided information such as contact forces. By allowing contacts between the deformable object and obstacles, we will show we increase the deformation space and we can efficiently handle constrained environments, i.e. having a very poor $\epsilon - \text{goodness}$ [8], and narrow passages by sliding along the contact space.

As we use two different models for dynamic simulation and static equilibrium configurations, it is necessary to fit models parameters in order to ensure their convergence at quasi-static configurations.

The paper is organized as follows. Section II presents both models used for dynamic simulation or static equilibrium configurations. Section III describes how to take advantage of both models using sampling-based methods to solve the motion planning problem for an extensible elastic rod. Finally, we evaluate in Section IV the method on several planning scenarios and discuss about the approach.

II. ELASTIC RODS MODELING

A. Extensible elastic rods Static Equilibrium Model (SEM)

The work from Bretl and McCarthy [5] offers a single global chart to describe the manifold of equilibrium configurations of an elastic rod. As coordinates in this chart are a subset of a low dimensional Euclidean space, it is especially well suited for sampling-based methods. However, this model only considers inextensible and non-shearable elastic rods. This section presents here an extension of [5] that enables us to derive a global parameterization for extensible and shearable elastic rods.

Consider a thin, naturally straight elastic rod in static equilibrium (i.e. the rod is motionless) held fixed at each end by robotic grippers. We may assume without loss of generality that the rod has unit length. With $t \in [0, 1]$ denoting arc-length along the rod, the position and orientation of the rod at arc-length t are described by an element $q(t)$ of the special Euclidean group $SE(3)$. The shape of the entire rod is described by a continuous map $q: [0, 1] \rightarrow SE(3)$. The rod is allowed to bend and twist, and the rod experiences axial extension and shear deformations. Therefore, the map

$q: [0, 1] \rightarrow SE(3)$ must satisfy

$$\dot{q} = q \left(\sum_{i=1}^6 u_i X_i + X_4 \right) \quad (1)$$

for some $u: [0, 1] \rightarrow \mathbb{R}^6$, where X_i with $i \in \{1, \dots, 6\}$ is a basis for the Lie algebra $\mathfrak{se}(3)$.

The functions $u_i: [0, 1] \rightarrow \mathbb{R}$ with $i \in \{1, \dots, 6\}$ are strains along the rod, where u_1 is the twisting strain, u_2 and u_3 are the bending strains, u_4 is the axial strain, and u_5 and u_6 are the shear strains. The functions q and u are referred to together as (q, u) .

The ends of the rod $q(0)$ and $q(1)$ are held by robotic grippers. Denote the set of all possible $q(0)$ by $\mathcal{B}_0 = SE(3)$ and the set of all possible $q(1)$ by $\mathcal{B}_1 = SE(3)$, i.e. \mathcal{B}_0 and \mathcal{B}_1 are the set of all possible placements of the robotic grippers holding the ends of the rod. Static equilibrium configurations of the rod are those which locally minimize the elastic potential energy stored in the rod. Assuming the elastic potential energy is quadratic in the strain functions and that twist, bending, stretching, and shear deformations are not coupled, the elastic potential energy is

$$\frac{1}{2} \int_0^1 \sum_{i=1}^6 c_i u_i^2 dt$$

where $c_1 > 0$ is the torsional stiffness, $c_2 > 0$ and $c_3 > 0$ are the bending stiffnesses, $c_4 > 0$ is the axial stiffness, and $c_5 > 0$ and $c_6 > 0$ are the shear stiffnesses of the rod. We say that (q, u) is a static equilibrium configuration of the rod if it is a local optimum of

$$\begin{aligned} & \underset{q, u}{\text{minimize}} && \frac{1}{2} \int_0^1 \sum_{i=1}^6 c_i u_i^2 dt \\ & \text{subject to} && \dot{q} = q \left(\sum_{i=1}^6 u_i X_i + X_4 \right) \\ & && q(0) = b_0, \quad q(1) = b_1 \end{aligned} \quad (2)$$

for some $b_0 \in \mathcal{B}_0$ and $b_1 \in \mathcal{B}_1$.

A similar optimal control formulation was used by Bretl and McCarthy to model an unsharable and inextensible elastic rod [5]. We now apply the procedure for deriving necessary and sufficient conditions for optimality outlined by [5] to the optimal control problem (2). Define the constants $c_{ij} = c_i^{-1} - c_j^{-1}$ for $i, j \in \{1, \dots, 6\}$. Theorem 1 provides necessary conditions for (q, u) to be a static equilibrium configuration of the rod.

Theorem 1: Define $\mathcal{A} = \mathbb{R}^6$. A trajectory (q, u) is a normal extremal of (2) for $b_0 = q(0)$ and $b_1 = q(1)$ if and only if there exists $\mu: [0, 1] \rightarrow \mathbb{R}^6$ satisfying

$$\begin{aligned} \dot{\mu}_1 &= c_{32} \mu_2 \mu_3 + c_{65} \mu_5 \mu_6 \\ \dot{\mu}_2 &= \mu_6 + c_{13} \mu_1 \mu_3 + c_{46} \mu_4 \mu_6 \\ \dot{\mu}_3 &= -\mu_5 + c_{21} \mu_2 \mu_1 + c_{54} \mu_4 \mu_5 \\ \dot{\mu}_4 &= c_3^{-1} \mu_3 \mu_5 - c_2^{-1} \mu_2 \mu_6 \\ \dot{\mu}_5 &= c_1^{-1} \mu_1 \mu_6 - c_3^{-1} \mu_3 \mu_4 \\ \dot{\mu}_6 &= c_2^{-1} \mu_2 \mu_4 - c_1^{-1} \mu_1 \mu_5 \end{aligned} \quad (3)$$

$$u_i = c_i^{-1} \mu_i \quad \text{for } i \in \{1, \dots, 6\} \quad (4)$$

and (1) with the initial condition $\mu(0) = a$ for some $a \in \mathcal{A}$.

Theorem 1 results from applying Theorem 3 of [5] to the optimal control problem (2). Theorem 3 of [5] relies on a geometric statement of the Pontryagin maximum principle, and the function $\mu: [0, 1] \rightarrow \mathbb{R}^6$ is the costate trajectory provided by the maximum principle. The function μ can also be interpreted as the vector of internal forces and torques acting along the rod [5].

Theorem 1 provides conditions under which (q, u) is a normal extremal of (2). Let \mathcal{C} denote the set of all smooth maps $(q, u): [0, 1] \rightarrow SE(3) \times \mathbb{R}^6$ which satisfy the necessary conditions given in Theorem 1. Then any $(q, u) \in \mathcal{C}$ is completely defined by the choice of $a \in \mathcal{A}$, as is the corresponding μ . Denote the resulting maps by $\Psi(a) = (q, u)$ and $\Gamma(a) = \mu$.

The trajectories $(q, u) \in \mathcal{C}$ are extrema of the optimal control problem (2). Theorem 2 provides a computational test to determine which of these extrema are local minima. This test relies on the theory of conjugate points in optimal control problems [1]. This defines the matrix \mathbf{G} by

$$\mathbf{G} = \text{diag}(c_1^{-1}, c_2^{-1}, c_3^{-1}, c_4^{-1}, c_5^{-1}, c_6^{-1})$$

Also define the matrix functions \mathbf{F} and $\mathbf{H}: \mathbb{R}^6 \rightarrow \mathbb{R}^{6 \times 6}$ by

$$\mathbf{F}(\mu) = \begin{bmatrix} 0 & c_{32}\mu_3 & c_{32}\mu_2 & 0 & c_{65}\mu_6 & c_{65}\mu_5 \\ c_{13}\mu_3 & 0 & c_{13}\mu_1 & c_{46}\mu_6 & 0 & 1+c_{46}\mu_4 \\ c_{21}\mu_2 & c_{21}\mu_1 & 0 & c_{54}\mu_5 & -1+c_{54}\mu_4 & 0 \\ 0 & -c_2^{-1}\mu_6 & c_3^{-1}\mu_5 & 0 & c_3^{-1}\mu_3 & -c_2^{-1}\mu_2 \\ c_1^{-1}\mu_6 & 0 & -c_3^{-1}\mu_4 & -c_3^{-1}\mu_3 & 0 & c_1^{-1}\mu_1 \\ -c_1^{-1}\mu_5 & c_2^{-1}\mu_4 & 0 & c_2^{-1}\mu_2 & -c_1^{-1}\mu_1 & 0 \end{bmatrix}$$

$$\mathbf{H}(\mu) = \begin{bmatrix} 0 & c_3^{-1}\mu_3 & -c_2^{-1}\mu_2 & 0 & 0 & 0 \\ -c_3^{-1}\mu_3 & 0 & c_1^{-1}\mu_1 & 0 & 0 & 0 \\ c_2^{-1}\mu_2 & -c_1^{-1}\mu_1 & 0 & 0 & 0 & 0 \\ 0 & c_6^{-1}\mu_6 & -c_5^{-1}\mu_5 & 0 & c_3^{-1}\mu_3 & -c_2^{-1}\mu_2 \\ -c_6^{-1}\mu_6 & 0 & 1+c_4^{-1}\mu_4 & -c_3^{-1}\mu_3 & 0 & c_1^{-1}\mu_1 \\ c_5^{-1}\mu_5 & -1-c_4^{-1}\mu_4 & 0 & c_2^{-1}\mu_2 & -c_1^{-1}\mu_1 & 0 \end{bmatrix}$$

Theorem 2: Let $(q, u) = \Psi(a)$ and $\mu = \Gamma(a)$ for some $a \in \mathcal{A}$. Let \mathbf{M} and $\mathbf{J}: [0, 1] \rightarrow \mathbb{R}^{6 \times 6}$ be the solutions of the linear, time-varying matrix differential equations

$$\frac{d\mathbf{M}}{dt} = \mathbf{F}(\mu(t))\mathbf{M} \quad \frac{d\mathbf{J}}{dt} = \mathbf{G}\mathbf{M} + \mathbf{H}(\mu(t))\mathbf{J} \quad (5)$$

with initial conditions $\mathbf{M}(0) = I$ and $\mathbf{J}(0) = 0$. Then, (q, u) is a local optimum of (2) for $b_0 = q(0)$ and $b_1 = q(1)$ if and only if $\det(\mathbf{J}(t)) \neq 0$ for all $t \in (0, 1]$.

Theorem 2 results from applying Theorem 4 of [5] to the optimal control problem (2). This Theorem provides a test to determine which extremals provided by Theorem 1 are local optima of (2), i.e. which $a \in \mathcal{A}$ produce local optima $\Psi(a) \in \mathcal{C}$. Let $\mathcal{A}_{\text{stable}} \subset \mathcal{A}$ be the subset of all $a \in \mathcal{A}$ which satisfy the conditions in Theorem 2, and let $\mathcal{C}_{\text{stable}} = \Psi(\mathcal{A}_{\text{stable}}) \subset \mathcal{C}$.

We now have a characterization of the set of all static equilibrium configurations of the rod. This allows us to use a sampling-based planning algorithm in which we directly sample static equilibrium configurations. This is done by sampling points in $\mathcal{A} = \mathbb{R}^6$, using the test in Theorem 2 to check if these points are members of $\mathcal{A}_{\text{stable}}$, and then evaluating the map $\Psi|_{\mathcal{A}_{\text{stable}}}: \mathcal{A}_{\text{stable}} \rightarrow \mathcal{C}_{\text{stable}}$ at these points.

B. The physical engine XDE

XDE offers a realistic multi-body dynamics simulation with various kinematics constraints (e.g. joints, kinematic loops) and with real-time performances. In addition to rigid bodies and kinematic chains, it can also handle DLOs, modeled as geometrically exact 3D beams [16]. This model enables large displacements thanks to Reissner kinematics and uses geometrically exact finite elements.

Furthermore, XDE can handle non-smooth contacts accurately with friction with constraints based methods. Also, it provides smooth bodies interactions mechanisms as Proportional-Derivative coupling for a given body position. This will be used for controlling rod grippers in simulation in the local planning method, as detailed in section III-B.

C. Model fitting between the SEM and XDE

For the purposes of this paper, we consider rods that are made from a homogeneous isotropic linear elastic material. As is common in mechanical engineering, XDE defines rod material elasticity parameters through Young's modulus E and shear modulus G . SEM stiffness coefficients c_i can then be deduced from elasticity parameters by $c_1 = GJ$, $c_2 = c_3 = EI$, $c_4 = EA$ and $c_5 = c_6 = GA$ where I represents the second moment of area, J the polar moment of inertia and A the cross-section area of the rod.

Using these parameters, we can bring simulated dynamic rods to quasi-static configurations described by the SEM by fitting rod grippers positions. As there exists a countable number of quasi-static configurations for grippers placements, this method does not give us the guarantee to fall into the desired local minimum of elastic energy. However, this will be sufficient to our needs and for keeping good exploration properties as explained in section IV-C. Attached video shows simulation results for models convergence.

III. MOTION PLANNING FOR EXTENSIBLE ELASTIC RODS

In this section, we show how the use of both models can improve the efficiency of solving our manipulation planning problem. By taking advantage of the parameterization provided by the SEM, we can sample quasi-static contact-free configurations that guide the exploration in the space of all admissible cable states reachable by the simulator.

A. Problem formulation

Consider a rod parameterized by $t \in [0, 1]$, its configuration $q(t)$ can be represented by the mapping $q: [0, 1] \rightarrow SE(3)$. The resulting configuration space would be a subset of the infinite-dimensional function space $C^\infty([0, 1], SE(3))$. In our case, the rod is discretized by the simulator using finite elements into $N - 1$ elements (thus N nodes), thus the resulting configuration space is a subset of $SE(3)^N$, where each configuration q is given by $q = (q_1 \ q_2 \ \dots \ q_N)^T$.

However, as we consider rod dynamics provided by the simulator, the phase space of the rod must be explored. Let $\mathcal{X} \subset (TSE(3))^N$, i.e. the tangent bundle associated to each

node configuration, be the state space of all rod states x satisfying elasticity constraints defined by $x = (q \ \dot{q})^T$.

Let now \mathcal{X}_{adm} be the closed set of all admissible states that can be reached by the dynamic simulator, which includes the set of states with contacts, and \mathcal{X}_{obs} the closed set of all states in collision with an obstacle. Note that $\mathcal{X}_{adm} = \mathcal{X} \setminus \text{int}(\mathcal{X}_{obs})$. The simulator, which relies on a state transition function, must guarantee that from any initial state in \mathcal{X}_{adm} , all states resulting for any input will be also in \mathcal{X}_{adm} .

However, the main drawback of considering the space of states reachable by a dynamic simulator is that we do not have a direct way to sample states on \mathcal{X} .

On the other hand, the result in section II-A has shown that all static equilibrium configurations of the rod can be parameterized using single chart mapping from a 6-dimensional Euclidean space \mathcal{A}_{stable} for a fixed rod base q_1 . Let now consider a free-flying quasi-static rod, its configuration space can be expressed using the same chart by $\mathcal{A}'_{stable} = SE(3) \times \mathcal{A}_{stable}$. The 12-dimensional submanifold of \mathcal{X} parameterized by this mapping is the open set \mathcal{Y} that describes all free-flying quasi-static elastic rods held by its both extremities, i.e. without contacts along the rod. Alternatively, the set \mathcal{Y} can be defined by

$$\mathcal{Y} = \{x \in \text{int}(\mathcal{X}_{adm}) \mid \dot{q} = 0\}$$

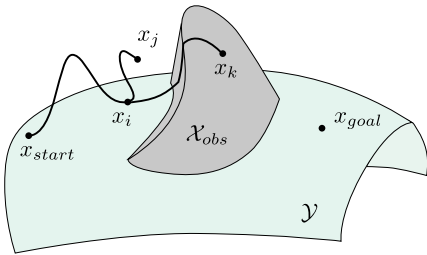


Fig. 2. Illustration of the tree exploration in the state space \mathcal{X}_{adm} while sampling states on the submanifold of quasi-static contact-free states \mathcal{Y} . We can see that the resulting state of an extension step can lie on this submanifold as x_i , be in contact as x_k or be any state in \mathcal{X}_{adm} as x_j .

Note that initial x_{start} and goal x_{goal} states of the problem lie in \mathcal{Y} . As shown in Figure 2, the key idea is to explore the space of all reachable states \mathcal{X}_{adm} while sampling states on the submanifold \mathcal{Y} using coordinates in \mathcal{A}'_{stable} .

B. Local planning using dynamics and contacts

In our context, the local planning problem consists in finding the trajectory from a given state $x_{from} \in \mathcal{X}_{adm}$ to a sampled state $x_{to} \in \mathcal{Y}$. There is various possible approaches and we describe in this subsection our controller that address that sub-problem.

We emphasize that taking advantage of contact information provided by the dynamic simulator by using contact sliding motions improves significantly the exploration of the search space for highly constrained cases (see section IV-C).

In this direction, we chose to exploit contact motions by not constraining the local planner trajectory on the submanifold \mathcal{Y} . Our method, detailed in Algorithm 1, consists in

a two steps approach as illustrated in Figure 3. First, the rod is manipulated by one of its gripper until the considered extremity reaches its goal position. Then, the other gripper is manipulated the same way while keeping the first one fixed.

Manipulation is done using a Proportional-Derivative controller on the grippers position. We also consider a time limit t_{max} , chosen at random between given bounds, for which the controllers are being applied for a given local planning instance.

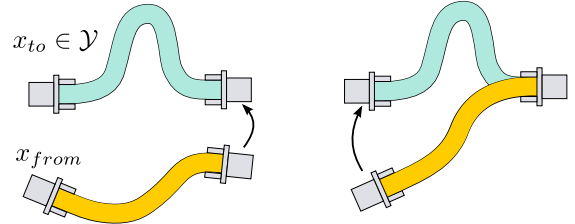


Fig. 3. Illustration of the two steps approach for the local planner from a state x_{from} to a quasi-static state x_{to} . First, a randomly chosen gripper is manipulated to its respective goal (left). Once its goal is reached, the first gripper is fixed and the other one is manipulated the same way (right).

Algorithm 1 EXTEND(x_{from}, x_{to})

Require: Time bounds $[T_{low}, T_{up}]$, simulation step time Δt

- 1: Select at random first gripper g_1
 - 2: Select at random a time limit $t_{max} \in [T_{low}, T_{up}]$
 - 3: $x_{new} \leftarrow x_{from}$
 - 4: **while** gripperDistance(x_{new}, x_{to}, g_1) > ϵ **and** $t < t_{max}$ **do**
 - 5: Apply position control on x_{new} at g_1 for Δt
 - 6: **end while**
 - 7: Let g_2 be other gripper
 - 8: **while** gripperDistance(x_{new}, x_{to}, g_2) > ϵ **and** $t < t_{max}$ **do**
 - 9: Apply position control on x_{new} at g_2 for Δt
 - 10: **end while**
 - 11: **return** x_{new}
-

C. Kinodynamic planning with sampling on a submanifold

Our approach to the manipulation planning problem for elastics rods is based on classical kynodynamic sampling-based approaches [10] as detailed in Algorithm 2. Some work has been done in sampling-based planning while projecting configurations on a constraint manifold as sampling strategy [4]. In our case, the complexity of the constraints based on the elasticity of the rod material make the formulation of a projector to the sampling submanifold a difficult task. However, the single global chart derived from the SEM that parameterize the submanifold \mathcal{Y} provides us a direct way to sample on the manifold and in particular offers the guarantee that it can be covered entirely through random sampling.

The pseudo-metric considered in the NEAREST returns an approximation of $\rho(a, b)$ is defined by

$$\rho(x_i, x_j) = \int_0^1 \|p_i(t) - p_j(t)\| dt \quad (6)$$

Algorithm 2 Kinodynamic RRT for an elastic rod with sampling on the quasi-static states submanifold

Require: Environment model, x_{start} , X_{goal}

- 1: Initialize the tree \mathcal{T} with x_{start}
 - 2: **while** \neg solved **and** $iter < N_{max}$ **do**
 - 3: $x_{rand} \leftarrow$ random quasi-static state $\in \mathcal{Y}$ or goal state
 - 4: $x_{near} \leftarrow$ NEAREST(\mathcal{T}, x_{rand})
 - 5: $x_{new} \leftarrow$ EXTEND(x_{near}, x_{rand})
 - 6: Add current state x_{new} to \mathcal{T}
 - 7: Add edge (x_{near}, x_{new})
 - 8: **end while**
-

where $p(t) \in \mathbb{R}^3$ is the translation part of the rod position at $q(t) \in SE(3)$. Intuitively, this pseudo-metric represents the swept surface area in the workspace between the two rod states as if all nodes could move in straight line which gives us a lower bound to the real swept surface area.

IV. RESULTS AND DISCUSSION

In this section, we will present our motivations to use dynamics and contacts and we will show and discuss some experimental results obtained in simulation.

A. A critical case: the double funnel

Consider a rod of length l and radius r , and the case of an environment with a very narrow passage for the given length. In the extreme case, this narrow passage would tend to have the shape of the rod, i.e. here a tunnel of length $l + \epsilon$ and of radius $2r + \epsilon$ as illustrated in Figure 4. Let X_{crt} be the set of rod configurations that are collision free when the rod is centered in the tunnel. As ϵ tends to zero, the set X_{crt} tends to be a unique state of with a zero volume. Consequently, the probability of sampling a state in X_{crt} tends to zero when the tunnel size tends to fit perfectly the rod shape.

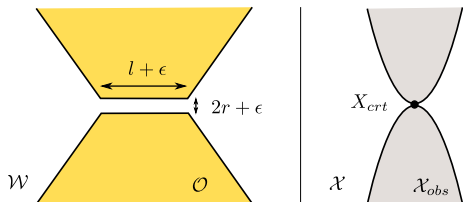


Fig. 4. A critical narrow passage for an elastic rod represented in the workspace \mathcal{W} (left) and its equivalent illustrated in rod state space \mathcal{X} . As ϵ tends to zero, the probability of sampling on X_{crt} also tends to zero.

This is an extreme narrow passage where sampling-based methods typically fail. The intuition behind taking advantage of contacts for this type of scenarios would be to:

- allow states to be in contact, i.e. $x \in \partial\mathcal{X}_{obs}$,
- being able to slide along contact boundary $\partial\mathcal{X}_{obs}$,
- being able to get off the contact.

Considering this, we tested our previously described approach on a *double funnel* scenario, with a tunnel of length $2l$ and a radius $3r$ (see Figure 5).

This type of case illustrate the advantage of our approach over classical collision-free sampling-based methods. On this

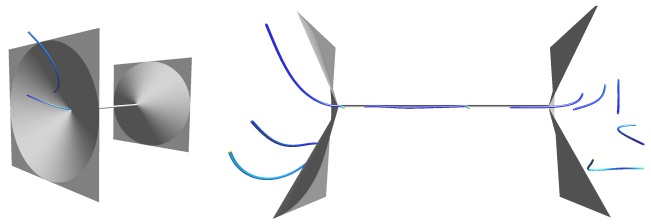


Fig. 5. The double funnel case where the elastic rod must go trough a very narrow passage (left) and a solution path (right) where the rod must go from the left side to the right side (view has been clipped for clarity).

scenario, a classical collision-free sampling-based method would typically fail (low probability to sample inside the tunnel). Our approach can solve the problem using dynamics/contacts with good performance results (see Tab. I).

B. Experimental results

A typical application to manipulation planning of elastic rods consists in assembly and disassembly studies of flexible parts such cables. In the case of disassembly study, the initial state is generally very constrained and the goal is a free region. Assembly studies can be solved by a symmetrical process. In addition to the *double funnel* case previously described, the following scenarios have been tested:

- *engine* (Figure 7) represents an industrial disassembly.
- *grid* (Figure 6) represents a disassembly operation for an elastic rod that is winded up into a grid.
- *powerplant* (Figure 1) where both initial and goal states for the elastic rod show a poor $\epsilon - goodness$.

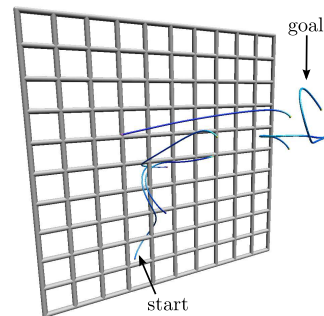


Fig. 6. Solution path on the "grid" scenario where the rod must go from a winded up state to a free state.

Solution paths on these scenarios are available in the attached video. Each scenario has been run 50 times with a limit in time of 20 minutes. All the benchmarks were run on a PC with 16GB of main memory and using one core of an Intel Core i7-2720QM processor running at 2.2GHz. Implementation has been done in C++ using the OMPL [17].

Results of the manipulation planning on previously presented scenarios are shown in Table I.

Assembly and disassembly scenarios showing difficult narrow passages are solved efficiently using our approach. In addition, we provide a solution path with accurate rod dynamics thanks to the simulation based on finite element

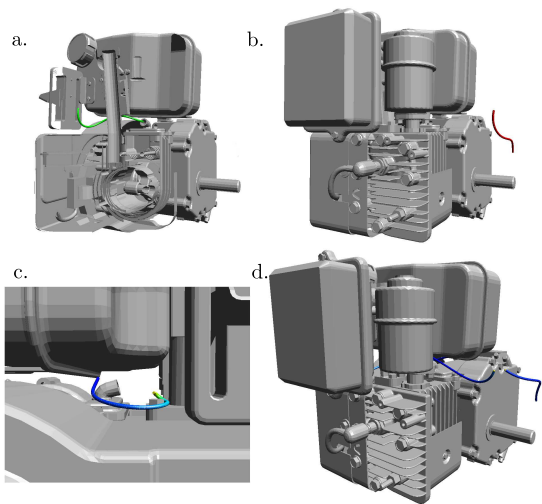


Fig. 7. Start (in green at clipped view a) and goal (in red at view b) states for the disassembly scenario "engine". The solution path makes use of contacts (views c and d).

TABLE I

KINODYNAMIC PLANNING FOR ELASTIC RODS WITH CONTACTS RESULTS

Scenario	Number of vertices / faces	Success rate	Resolution time (sec) avg \pm std. dev
double funnel	198/388	100%	77.2 \pm 36.0
grid	704/1320	96%	34.4 \pm 25.5
engine	64885/131583	94%	119.6 \pm 109.3
powerplant	24870/20053	31%	402.5 \pm 293.6

analysis. This solution includes the sequence of controls that should be applied to the rod to solve the problem, and this information could be used in realistic conditions.

Note that the planner performance significantly decreases with the *powerplant* scenario, as it differs from typical assembly studies and consists in a complex and highly constrained case from initial to goal states.

C. Discussion about completeness

As our approach relies on sampling on a submanifold of the state space, our algorithm is probabilistically complete in the sampled submanifold \mathcal{Y} . Indeed, our direct sampling method enables us to cover the entire submanifold \mathcal{Y} of quasi-static contact-free configurations through the sampling the process. Furthermore, each infinitesimally small quasi-static motion that lies entirely in the submanifold \mathcal{Y} can be achieved through dynamic simulation as both models fit.

Also, there exists a countable number of static equilibrium rod configurations for given grippers placement, the local planner may fail to reach the desired state by uniquely controlling grippers positions and fall into another local minimum of elastic energy. For the purpose of our local method, this does not invalidate the probabilistic completeness of the approach as there is a non null probability to reach the desired state. Moreover, these configurations are guaranteed to be close with respect to our metric, which enables us to keep a good Voronoi bias in \mathcal{Y} . For this reason, we

first limited our goal region X_{goal} to the set of all static equilibrium configurations for given grippers positions.

V. CONCLUSION

In this paper, we proposed an approach to the manipulation planning problem of an extensible elastic rod in collision-free or contact space. We showed that by using a static equilibrium model, we can efficiently sample on the submanifold of its quasi-static contact-free states whereas the kinodynamic planning algorithm uses dynamic simulation and explore the full state space of the rod. Thanks to dynamic simulation, the planning algorithm can take advantage of contacts by allowing sliding motions in order to solve difficult narrow passages, where collision-free typical sampling-based method would fail.

ACKNOWLEDGMENT

This work was supported by the French National Research Agency under the project Flecto (ANR- Digital Models). The *engine* industrial model is courtesy of Siemens-KineoCAM.

REFERENCES

- [1] A.A. Agrachev and Y.L. Sachkov. Control theory from the geometric viewpoint. *Springer, Berlin*, 2004.
- [2] N.M. Amato and Y. Wu. A randomized roadmap method for path and manipulation planning. In *IEEE Int. Conf on Robotics and Automation*, pages 113–120 vol.1, 1996.
- [3] O. B. Bayazit, J.-M. Lien, and N. M. Amato. Probabilistic roadmap motion planning for deformable objects. In *IEEE Inter. Conf. on Robotics and Automation*, pages 2126–2133, 2002.
- [4] D. Berenson, S. Srinivasa, D. Ferguson, and J. J. Kuffner. Manipulation planning on constraint manifolds. In *IEEE Inter. Conf. on Robotics and Automation*, pages 625–632, 2009.
- [5] T. Bretl and Z. McCarthy. Quasi-static manipulation of a kirchhoff elastic rod based on a geometric analysis of equilibrium configurations. *I. J. Robotic Res.*, 33(1):48–68, 2014.
- [6] R. Gayle, P. Segars, M. C. Lin, and D. Manocha. Path planning for deformable robots in complex environments. In *Robotics: Science and Systems*, pages 225–232. The MIT Press, 2005.
- [7] I. Kabul, R. Gayle, and M. C. Lin. Cable route planning in complex environments using constrained sampling. In *ACM Symposium on Solid and Physical Modeling*, pages 395–402, 2007.
- [8] L. E. Kavraki, J.-C. Latombe, R. Motwani, and P. Raghavan. Randomized query processing in robot path planning (extended abstract). In *Jour. of Computer and System Sciences*, pages 353–362, 1995.
- [9] F. Lamiroux and L. E. Kavraki. Planning paths for elastic objects under manipulation constraints. *I. J. Robotic Res.*, 20(3):188–208, 2001.
- [10] S. M. LaValle and J. J. Kuffner. Randomized kinodynamic planning. *I. J. of Robotics Research*, 20(5):378–400, May 2001.
- [11] M. Moll and L. E. Kavraki. Path planning for deformable linear objects. *IEEE Transactions on Robotics*, 22:625–636, 2006.
- [12] S. Rodríguez, J.-M. Lien, and N. M. Amato. Planning motion in completely deformable environments. In *IEEE ICRA*, pages 2466–2471, 2006.
- [13] O. Roussel, M. Taïx, and T. Bretl. Efficient motion planning for quasi-static elastic rods using geometry neighborhood approximation. In *IEEE/ASME Int. Conf. on Advanced Intelligent Mechatronics*, 2014.
- [14] M. Saha and P. Isto. Manipulation planning for deformable linear objects. *IEEE Transactions on Robotics*, 23(6):1141–1150, Dec 2007.
- [15] T. Siméon, J.P. Laumond, J. Cortes, and A. Sahbani. Manipulation planning with probabilistic roadmaps. *I. J. Robotics Res.*, 23(7-8), 2004.
- [16] JC Simo. A finite strain beam formulation. the three-dimensional dynamic problem. part i. *Computer methods in applied mechanics and engineering*, 49(1):55–70, 1985.
- [17] I. A. Sucan, M. Moll, and L. E. Kavraki. The open motion planning library. *IEEE Robot. Automat. Mag.*, 19(4):72–82, 2012.
- [18] H. Wakamatsu and S. Hirai. Static modeling of linear object deformation based on differential geometry. *I. J. Robotic Res.*, 23(3):293–311, 2004.